

Shape Variation of Linear Polymers upon Phase Separation in a Ternary Solution

Lei Guo and Erik Luijten*

Department of Materials Science and Engineering,
University of Illinois at Urbana–Champaign,
1304 West Green Street, Urbana, Illinois 61801

Received April 18, 2003

Revised Manuscript Received August 14, 2003

Introduction

It was recognized by Kuhn 70 years ago that the typical shape of a flexible polymer chain is ellipsoidal rather than spherical.¹ This shape anisotropy, besides being a fundamental property, is of considerable scientific and technological importance, affecting a variety of polymer properties. For example, it has been proposed that it influences the flow properties of polymeric fluids,² and recently it was demonstrated³ that the polymer asphericity can account for the polymer-induced depletion potential observed in colloid–polymer mixtures.⁴ Accordingly, the shape of random-walk (RW) and self-avoiding-walk (SAW) polymers has been studied extensively both analytically and by simulations.^{5–9} Very recently, the asymmetric shape has actually been observed in experiments.^{10,11}

However, it should be noted that the experiments, as well as the vast majority of the theoretical work, focus on the shape of a single coil in a highly dilute solution. Studies of the role of concentration are rare and have essentially shown that, for a homogeneous solution of athermal chains, the asphericity diminishes only very slowly upon increasing concentration.^{12,13} In a poor solvent, the reverse effect was observed,¹⁴ which is essentially due to the coil–globule transition taking place in the polymer-lean phase. Clearly, structural and thermodynamic properties are intimately connected, which has motivated us to investigate shape variations within a more complicated phase diagram.

In this Note, we discuss the coil shapes of polymers in a *ternary solution*, consisting of two polymer species (denoted by A and B) and a solvent (S). In particular, we focus on the effect of polymer–polymer separation in this system, which we have investigated by means of Monte Carlo simulations. It is found that this phase transition indeed has a dramatic effect on the polymer shape, which is characterized by the eigenvalues $\lambda_1 \leq \lambda_2 \leq \lambda_3$ of the radius-of-gyration tensor \mathbf{Q} , defined as^{5,15}

$$Q_{\alpha\beta} = \frac{1}{2N^2} \sum_{i,j=1}^N [r_{i,\alpha} - r_{j,\alpha}][r_{i,\beta} - r_{j,\beta}] \quad (1)$$

where \mathbf{r}_i represents the position of the i th monomer along the chain, $\alpha, \beta = 1, 2, 3$ denote Cartesian components, and N is the degree of polymerization of the polymer. The sum of the three eigenvalues equals the squared radius of gyration R_g^2 . An important measure is the asphericity A .^{6,9,16,17}

$$A = \frac{1}{2} \left(\frac{(\lambda_1 - \lambda_2)^2 + (\lambda_2 - \lambda_3)^2 + (\lambda_3 - \lambda_1)^2}{(\lambda_1 + \lambda_2 + \lambda_3)^2} \right) \quad (2)$$

* Corresponding author. E-mail: luijten@uiuc.edu.

where the brackets indicate the ensemble average.¹⁸ A takes values between 0 (sphere) and 1 (rod). In the dilute limit it approaches a universal value for $N \rightarrow \infty$, estimated as 0.415 from first-order ϵ expansions and as 0.431 from simulations.^{9,19,20} In the melt limit, where the chains behave ideally, this value is anticipated to decrease to the (exactly known) RW value 0.39427....¹⁷

Simulation Model and Techniques

We have performed Monte Carlo simulations for the bond fluctuation model (BFM),^{21,22} with chains containing up to 80 units (each unit corresponds to a Kuhn segment of 3–5 monomers). One of the advantages of the BFM is the large number of available bond angles, permitting a more realistic modeling of flexible chains than is possible with random-walk models. To prevent interference of polymer–solvent (PS) and polymer–polymer (PP) phase separation, the polymer–solvent coexistence curve was suppressed by setting the interactions among units of the same type as well as the polymer–solvent interactions to zero: $\epsilon_{AA} = \epsilon_{BB} = \epsilon_{SS} = \epsilon_{AS} = \epsilon_{BS} = 0$.²³ Thus, the PP separation is driven by a repulsive square-well interaction among unlike segments, ϵ_{AB} , which can be identified with a (reduced) inverse temperature scale $1/k_B T$, where we will set $k_B = 1$. Further details of the BFM are described in ref 24.

For simplicity, we have studied symmetric, monodisperse systems, $N = N_A = N_B$. This enabled us to increase the simulation efficiency via semi-grand-canonical (SGC) moves,²⁵ in which only the “identity” of a chain is changed; as an additional advantage, PP phase coexistence by necessity occurs for identical chemical potentials. Thus, the concentrations of A and B polymers fluctuate in the course of the simulation but on average are equal. The SGC moves were combined with local monomer moves and reptation-like moves. The overlap threshold (discussed below) was determined via grand-canonical moves that employed a variant of the recoil-growth scheme.^{26,27} Properties were sampled every 50 sweeps; the systems were equilibrated for 4000 such samples, followed by 100 000 production samples per state point.

Results and Discussion

The location of the A–B demixing curve depends on the total monomer concentration ϕ and on the degree of polymerization. Owing to the intrinsic symmetry of our systems, the phase diagram is symmetric in the order parameter. Figure 1 shows the cross section of the phase diagram corresponding to the critical plane, for three different chain lengths. For each chain length, the phase diagram contains two critical lines, denoted a and b in the figure. Line b indicates the critical transition in the semidilute regime. Flory–Huggins theory predicts this line to have a linear dependence on concentration,²⁸ whereas our results exhibit a manifestly nonlinear ϕ dependence, in agreement with renormalization-group predictions and earlier numerical findings.^{29–32} Furthermore, de Gennes³³ has predicted that ternary mixtures do not exhibit PP demixing for concentrations below the overlap concentration ϕ^* separating the dilute from the semidilute regime and that symmetric mixtures undergo a critical phase transition at ϕ^* . Both predictions have been confirmed by our simulations;³²

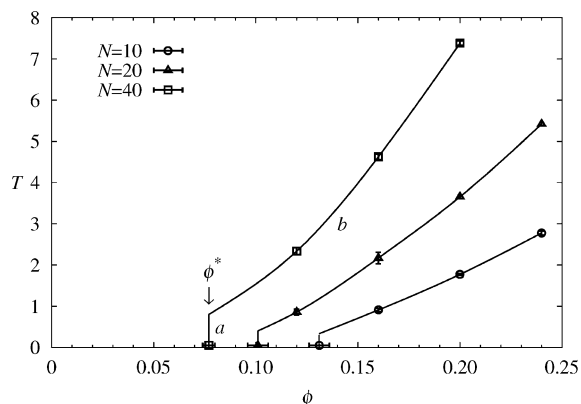


Figure 1. Critical cross section of the phase diagram for ternary mixtures with chain lengths $N = 10, 20,$ and 40 . The curves indicate the critical temperature for polymer–polymer demixing as a function of total monomer concentration ϕ and thus separate the mixed and the demixed phases. Note the sharp drop in critical temperature for concentrations below the overlap threshold ϕ^* . For clarity, the curves a and b and the overlap threshold have only been labeled for $N = 40$. The lines are guides to eyes.

the continuous phase transition at the overlap threshold is indicated by line a in Figure 1. For completeness, we note that the transition becomes first-order in the case of unequal chemical potentials for the A and B polymers.

We now proceed to study the shape variation of individual polymer chains within this phase diagram by considering an isotherm that intersects the critical line a in Figure 1. The correspondingly low temperature merely affects the strength of the repulsion between unlike monomers, since identical monomers only experience an excluded-volume interaction (owing to our choice of the interaction parameters).³⁴ The top panel of Figure 2 shows the asphericity A as a function of ϕ for $N = 40$. The dashed curve refers to a homogeneous athermal solution and shows a weak decrease of asphericity with increasing concentration: The screening of the excluded-volume interaction restores the polymers to a more spherical shape; a similar effect is responsible for the difference between RW and SAW chains observed under dilute conditions.^{6,9} For very low concentrations, the data for the ternary solution coincide with this reference curve because very few A–B interactions will be present. As ϕ increases in the mixed phase (i.e., $\phi < \phi^*$), the strong repulsion between unlike polymers induces a significant decrease of the asphericity. At $\phi = \phi^*$ phase separation sets in, leading to a branch point in the graph for the asphericity. For the majority component, the diminishing repulsion more than compensates the effect of increasing concentration, leading to an initial upward trend for the asphericity. At sufficiently high concentrations, phase separation is virtually complete, and A decreases again, coinciding with the athermal reference curve. The minority component, on the other hand, experiences a dramatic decrease in asphericity for $\phi > \phi^*$, caused by the strong repulsion exerted by the chains belonging to the majority species. This tendency is only reinforced by the increasing concentration, resulting in values for A that are similar to those observed near the coil–globule transition in dilute solutions.¹⁴ The decrease of A for the minority component is reflected in the behavior of R_g^2 (middle panel of Figure 2), which, upon phase separation, drops to $R_g^2 \approx 15$ at $\phi = 0.16$. This small value of R_g^2 for chains with 40 repeat units clearly

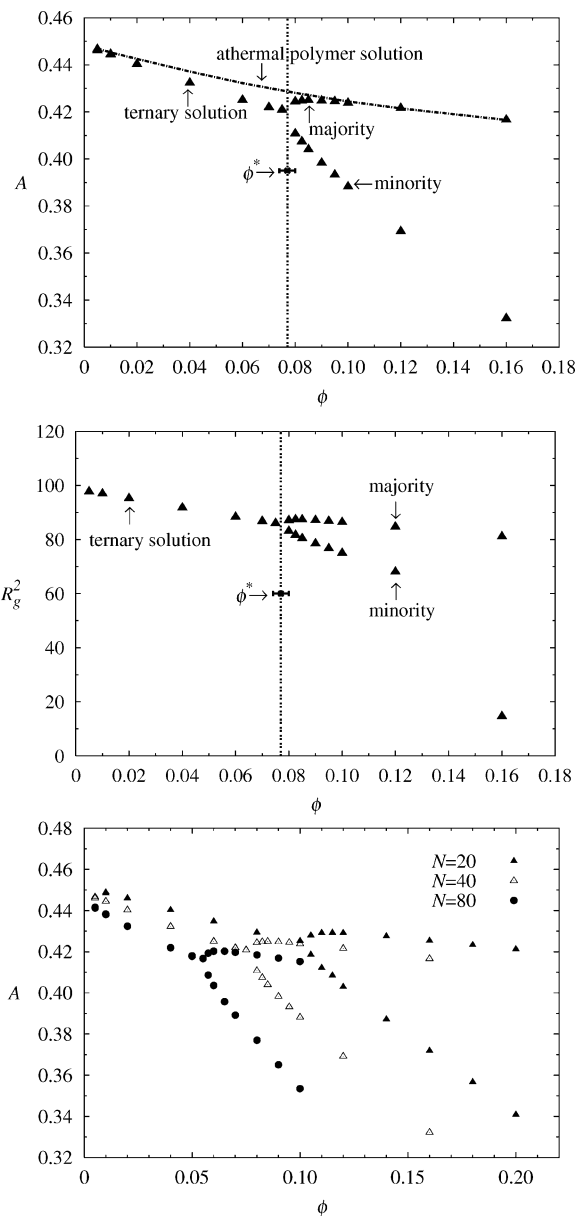


Figure 2. (top) Asphericity for $N = 40$ as a function of concentration for a ternary solution at a low temperature (triangles) and for a homogeneous athermal polymer solution (dashed line). Upon phase separation, the minority component experiences a large decrease in asphericity. (middle) The corresponding change of the squared radius of gyration for both majority and minority components. The decrease in asphericity for the minority component coincides with a rapid decrease in the radius of gyration. (bottom) Asphericity as a function of concentration for three different chain lengths. All chain lengths exhibit qualitatively similar behavior, where the shift to lower concentrations reflects the decrease of the overlap threshold with increasing degree of polymerization.

indicates the collapse of the minority chains, leading to the large decrease in A .

The effect of the chain length on A is illustrated in the bottom panel of Figure 2, where the data for $N = 40$ are shown together with those for $N = 20$ and $N = 80$. All data were obtained along the same isotherm. For each chain length, the branch point corresponds to the respective overlap concentration ϕ^* (cf. Figure 1 for $N = 20$ and $N = 40$). While the results are qualitatively similar, there is a slight decrease in A with increasing N at very low concentrations, in accordance with the

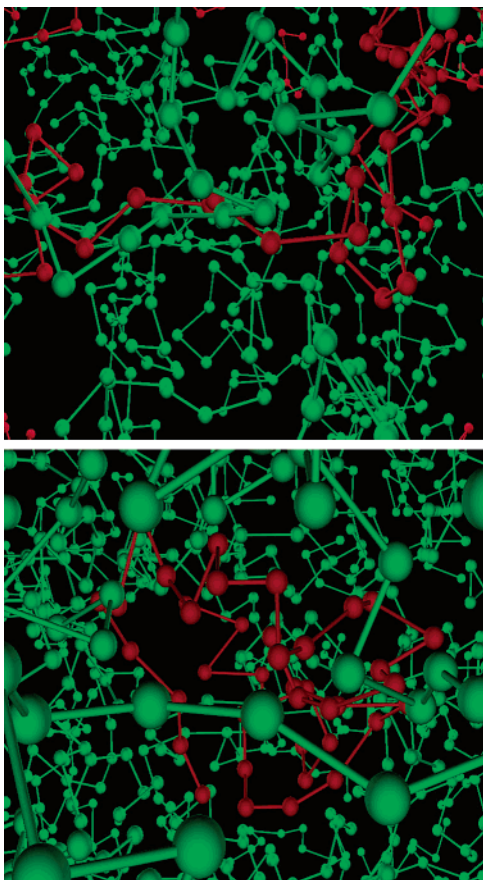


Figure 3. Snapshots of a ternary polymer solution at $T = 0.2$. Top: $\phi = 0.07$, i.e., no phase separation. Chains of both types have the same elongated shape. Bottom: $\phi = 0.1$, where phase separation has set in. The red chain belongs to the minority component in the selected phase and clearly has adopted a much more spherical conformation.

prediction that this quantity should approach a universal limiting value near 0.431.⁹

The dramatic change of the shape of the minority component upon phase separation is illustrated in Figure 3. The top panel shows a typical chain of type B (red) in a system with $N = 40$ and $\phi = 0.07$ (i.e., in the mixed phase). A region with relatively few B chains was chosen for contrast, but the selected chains have a representative shape. In the bottom panel, phase separation has been induced by increasing the total monomer concentration to $\phi = 0.1$, where the ratio of the number of majority (A) and minority (B) chains is about 27. The contraction of the B chains, resulting from the repulsion of the A chains (green), is clearly visible.

The values for the asphericity only represent ensemble averages, whereas knowledge of the underlying distribution functions $P(A)$ is relevant as well. For example, in ref 3 an optimal data description was obtained for an admixture of polymers of various shapes. Figure 4 shows $P(A)$ at various ϕ for both the majority and the minority component. For $\phi < \phi^* \approx 0.077$, where both distributions necessarily coincide, a wide variety of shapes occurs. After phase separation, however, $P(A)$ for the minority component develops a peak near $A = 0.2$. The peak position corresponds to a fast decrease in $P(A)$ for the majority component. The latter behavior has been observed before for a single SAW polymer^{9,35} and seems robust. However, the precise reason for the sudden change near $A = 0.2$ still remains an open question.

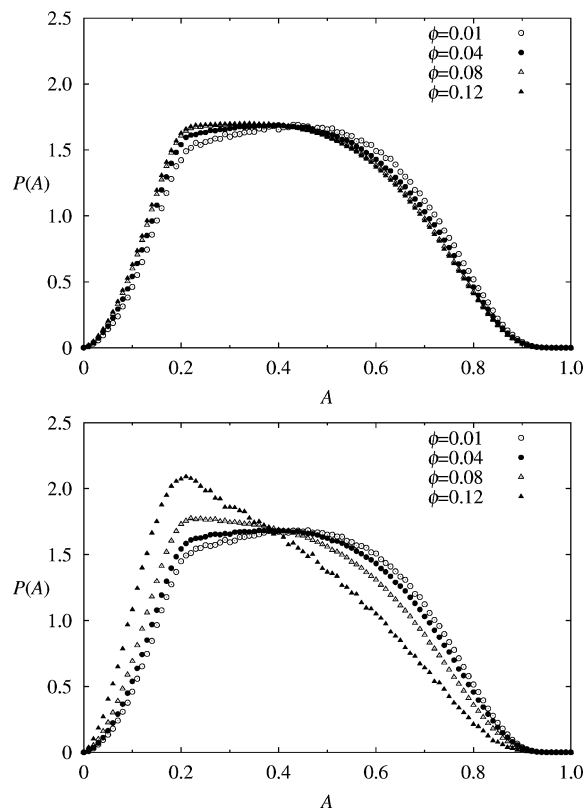


Figure 4. Probability distribution of the asphericity A for $N = 40$ at $T = 0.2$, for various concentrations ϕ . (top) Distribution for the majority component. The broad distribution reflects the wide range of conformations present. (bottom) Distribution for the minority component. Already slightly above the overlap threshold, this distribution has developed a sharp peak at low asphericity.

Conclusions

The shape of linear, flexible polymers in ternary solutions has been studied by means of Monte Carlo simulations for the bond fluctuation model, under conditions where both polymer components dissolve well in the solvent. At very low concentrations our results are consistent with the results for a single SAW polymer, reconfirming the universality of the shape properties. Upon polymer–polymer demixing, the shape of the minority component in the separated phases changes dramatically, owing to the repulsion exerted by surrounding polymers. This change is similar to that observed for polymers in a poor solvent. Further simulations have shown that comparable results are obtained along isotherms at higher temperatures and for systems in which the PS demixing is not suppressed.³² In ternary systems where the solvent quality is poor for either or both of polymers, polymer–polymer demixing at the overlap threshold will be preempted by polymer–solvent separation.²⁷

Acknowledgment is made to the donors of the American Chemical Society Petroleum Research Fund for support of this research through Grant 38543-G7. The authors thank M. Müller for generously providing parts of the simulation code and K. Schweizer for helpful comments. Computing support by the Materials Computation Center (National Science Foundation Grant DMR-99-76550) is gratefully acknowledged.

References and Notes

- (1) Kuhn, W. *Kolloid-Z.* **1934**, *68*, 2.

- (2) Abernathy, F. H.; Bertschy, J. R.; Chin, R. W.; Keyes, D. E. *J. Rheol.* **1980**, *24*, 647.
- (3) Triantafillou, M.; Kamien, R. D. *Phys. Rev. E* **1999**, *59*, 5621.
- (4) Verma, R.; Crocker, J. C.; Lubensky, T. C.; Yodh, A. G. *Phys. Rev. Lett.* **1998**, *81*, 4004.
- (5) Šolc, K. *J. Chem. Phys.* **1971**, *55*, 335.
- (6) Aronovitz, J. A.; Nelson, D. R. *J. Phys. (Paris)* **1986**, *47*, 1445.
- (7) Rudnick, J.; Gaspari, G. *Science* **1987**, *237*, 384.
- (8) Bishop, M.; Saltiel, C. J. *J. Chem. Phys.* **1986**, *85*, 6728.
- (9) Jagodzinski, O.; Eisenriegler, E.; Kremer, K. *J. Phys. I* **1992**, *2*, 2243.
- (10) Haber, C.; Ruiz, S. A.; Wirtz, D. *Proc. Natl. Acad. Sci. U.S.A.* **2000**, *97*, 10792.
- (11) Maier, B.; Rädler, J. O. *Macromolecules* **2001**, *34*, 5723.
- (12) Bishop, M.; Ceperley, D.; Frisch, H. L.; Kalos, M. H. *J. Chem. Phys.* **1980**, *72*, 3228.
- (13) Olaj, O. F.; Petrik, T.; Zifferer, G. *Macromol. Theory Simul.* **1997**, *6*, 1277.
- (14) Szleifer, I. *J. Chem. Phys.* **1990**, *92*, 6940.
- (15) Rudnick, J.; Gaspari, G. *J. Phys. A* **1986**, *19*, 191.
- (16) Gaspari, G.; Rudnick, J.; Beldjenna, A. *J. Phys. A* **1987**, *20*, 3393.
- (17) Diehl, H. W.; Eisenriegler, E. *J. Phys. A* **1989**, *22*, L87.
- (18) Historically, this average has been approximated by the ratio of the separate expectation values of the numerator and the denominator. However, this quantity has been shown to underestimate the effect of monomer interactions.^{9,16,17,20}
- (19) Bishop, M.; Saltiel, C. J. *J. Chem. Phys.* **1988**, *88*, 6594.
- (20) Cannon, J. W.; Aronovitz, J. A.; Goldbart, P. *J. Phys. I* **1991**, *1*, 629.
- (21) Carmesin, I.; Kremer, K. *Macromolecules* **1988**, *21*, 2819.
- (22) Deutsch, H. P.; Binder, K. *J. Chem. Phys.* **1991**, *94*, 2294.
- (23) Further simulational details will be provided in a forthcoming publication.³²
- (24) Wilding, N. B.; Müller, M.; Binder, K. *J. Chem. Phys.* **1996**, *105*, 802.
- (25) Sariban, A.; Binder, K. *J. Chem. Phys.* **1987**, *86*, 5859.
- (26) Consta, S.; Wilding, N. B.; Frenkel, D.; Alexandrowicz, Z. *J. Chem. Phys.* **1999**, *110*, 3220.
- (27) Luijten, E.; Wilding, N. B.; Guo, L., manuscript in preparation.
- (28) Flory, P. J. *Principles of Polymer Chemistry*; Cornell University Press: Ithaca, NY, 1953.
- (29) Schäfer, L.; Kappeler, C. *J. Phys. (Paris)* **1985**, *46*, 1853.
- (30) Broseta, D.; Leibler, L.; Joanny, J.-F. *Macromolecules* **1987**, *20*, 1935.
- (31) Sariban, A.; Binder, K. *J. Colloid Polym. Sci.* **1994**, *272*, 1474.
- (32) Guo, L.; Luijten, E., to be published.
- (33) de Gennes, P.-G. *Scaling Concepts in Polymer Physics*; Cornell University Press: Ithaca, NY, 1979.
- (34) To ensure that the low temperature does not lead to ergodicity problems, we have verified that single chains diffuse freely during the simulation.
- (35) Zifferer, G. *J. Chem. Phys.* **1998**, *109*, 3691.

MA034506O